Science World Journal Vol. 18(No 4) 2023
www.scienceworldjournal.org
ISSN: 1597-6343 (Online), ISSN: 2756-391X (Print)
Published by Faculty of Science, Kaduna State University
DOI: https://dx.doi.org/10.4314/swj.v18i4.22

Full Length Research Article

STATISTICAL OPTIMIZATION OF IODINE ADSORPTION FOR *PENTACLETHRA MACROPHYLLA* PODS ACTIVATED CARBON PRODUCTION

* [1,2]Gabriel O. Ogbeh, [2]Ayodele O. Ogunlela, and [1]Nicholas O. Emaikwu

[1]Department of Agricultural and Environmental Engineering, Joseph Sarwuan Tarka University, P.M.B. 2373 Makurdi, Nigeria
[2]Department of Agricultural and Biosystems Engineering, University of Ilorin, Nigeria

*Corresponding Author Email Address: gabriel.ogbeh@uam.edu.ng Phone: +2348038635582

ABSTRACT
Efficient production of activated carbon (AC) depends on variables such as feedstock properties, preparation conditions, and activating agents. This study aimed to identify optimal conditions for AC production from African Oil Bean (*Pentaclethra macrophylla*) Pods (PMps) using potassium hydroxide (KOH) and phosphoric acid (H_3PO_4) as activating agents. Through a systematic iodine adsorption characterization approach and leveraging Response Surface Methodology as a chemometric tool, the study fine-tuned chemical activation and carbonization parameters (temperature, time, and impregnation ratio) for producing PMACs. The adjustments directly impacted the iodine number (I_n) and yields (C_y) of the PMACs (PMAC-KOH_{op} and PMAC-H_3PO_{4op}). The predicted I_n and C_y values closely aligned with the observed values – (PMAC-KOH_{op}: 918.58 mg/g predicted vs. 916.56 mg/g observed; PMAC-H_3PO_{4op}: 593.44 mg/g predicted vs. 592.88 mg/g observed) and (PMAC-KOH_{op}: 39.60% predicted vs. 39.15% observed; PMAC-H_3PO_{4op}: 51.30% predicted vs. 51.10% observed), demonstrating precision of the production process. Key structural properties, including BET specific surface areas (SSA), total pore volumes (V_t), and average pore diameters, exhibited notable differences between the PMAC-KOH_{op} and PMAC-H_3PO_{4op}, with the former demonstrating superiority. Particularly, FTIR spectra highlighted higher aromaticity in PMAC-KOH_{op}, revealing the preference for KOH over H_3PO_4 in the chemical activation of PM_{ps}. The high I_n achieved with the PMAC-KOH_{op} indicated its efficacy as a pollutant adsorbent, aligning with the established attributes of commercial granular activated carbons for pollutants removal from wastewater. This study establishes PMps as a dependable AC precursor, emphasizing the advantages of KOH over H_3PO_4 in chemical activation. Future research should be directed at investigating PMAC-KOH_{op} adsorption capabilities for diverse pollutants and exploring PMps' potential contributions to metallic or nanocomposite formations with other adsorbents.

Keywords: Activated carbons; Adsorbent; Chemical activation; Chemometric tool; Iodine number; *Pentaclethra macrophylla* Pods

Graphical Abstract

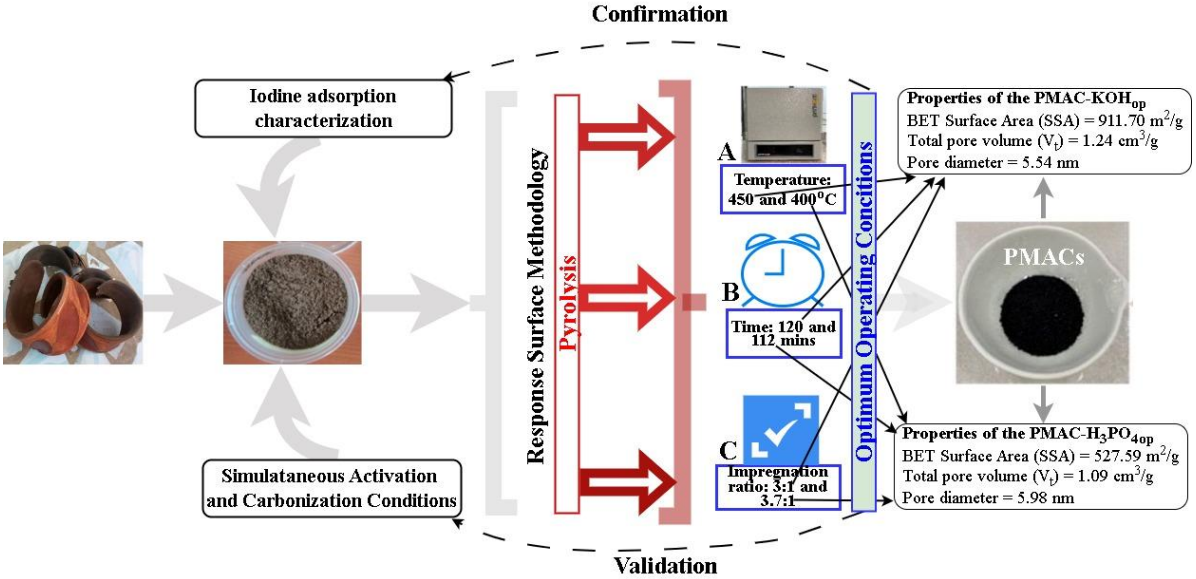

Highlights

- KOH and H_3PO_4 were utilised as activators to produce PMACs with iodine adsorption characterization.
- Over 68% of the volatile matter and 74% of moisture in the PM_{ps} were burnt off during carbonization.
- The ACs demonstrated graphitic features but their properties differ from each other.

- Both ACs produced were of the mesoporous average pore diameter range–2≥PMACs≤50 nm.
- The PMAC-KOH_{op} has superior properties with 916.56 mg/g I_n and 911.70m^2/g BET SSA area.

INTRODUCTION

Activated carbon (AC) is a porous material synthesized from carbonaceous feedstock through an activation process, resulting in the creation of minuscule gaps between the carbon atoms (Ravichandran et al., 2018). Alternatively, some perspectives defined AC as a category of carbon-based material without a specific structural formula or chemical analysis (Ngueabouo et al., 2022). Regardless of the definition, activated carbons (ACs) generally exhibit superior porosity and extensive interparticle surface area, making them highly sought after for various industrial applications (Vunain et al., 2021). Their exceptional adsorptive capacity, mostly based on such characteristics as large specific surface area, superior porosity, structural stability, and surface functional groups (Xu et al., 2023), positions them as the most utilized adsorbents for tasks ranging from energy storage to removal of organic and inorganic chemical pollutants in both liquid and gaseous phases. Conventionally, most commercial activated carbons are synthesized from non-renewable sources like petroleum, coal, coke, peat, and refinery residues (Ravichandran et al., 2018; Zieliński et al., 2022), which are contributing to concerns about their high costs and dwindling reserves. This situation is particularly pronounced in developing countries. To address these challenges, there is a growing emphasis on exploring low-cost, carbon-rich materials that can serve as alternatives for producing high-performing activated carbons. This pursuit aims to mitigate the limitations associated with conventional precursors and foster sustainable practices in activated carbon production (Ajaelu *et al*., 2022; Nindjio *et al*., 2022).

The production of AC is influenced by three categories of factors, namely, the feedstock properties, the preparation conditions, and the activating agents used (Kwiatkowski and Broniek, 2017; Li *et al*., 2017). Generally, activated carbons may be produced by physical activation method, which involves carbonization and activation of the feedstock in two steps, with gases such as CO_2, O_2, or steam serving as the activating agent (Ogungbenro *et al*., 2017; Yang *et al*., 2010); or by chemical activation method, which transforms cellulose structures into carbonaceous material through simultaneous dehydration and carbonization, with strong base, acid, or salt serving as the activating agent (Jaria et al., 2019; Yorgun and Yildiz, 2015); or by combined physical and chemical activation method, or by microwave-assisted activation method (Ao et al., 2018; Lam et al., 2017; Liew et al., 2018). The chemical activation method offers the advantage of allowing the production of activated carbons of higher qualities at lower cost due to its lower energy requirement to generate the needed activation temperature, typically ranging from 400 to 700^oC (Loredo-Cancino *et al*., 2013). This method is, however, beset with the challenge of selecting the most appropriate operating conditions required to produce ACs of desired qualities. Lower or excessive utilization of the operating conditions for chemical activation of the precursor during AC production have several implications. For instance, excessive activation temperature may result in the widening of micropores. While micropores are desirable for adsorption, too much widening can affect the specific adsorption properties of the AC (Yashim et al., 2016). High temperatures can also lead to burn-off, reducing the AC mass, potentially affecting the final product's properties (Yashim et al., 2016). An increase in impregnation ratio, particularly with activating agents like KOH or H_3PO_4, can result in a gradual decrease in the yield of AC (Zakaria et al., 2021). The impregnation ratio significantly influences the development of pores in AC, with higher ratios enhancing pore development but potentially causing pores to collapse and impacting porosity (Putranto et al., 2022). Depending on the content, stability, presence of heteroatoms, and functional groups within the precursor, ACs of different characteristics can be produced (Ekpete *et al*., 2017; Hidayu and Muda, 2016; Shamsuddin *et al*., 2016). Several agroforestry residues have been explored for their potential as AC precursors. But the quality of the ACs finally produced from most agroforestry residues depends heavily on the activation process and adsorption method applied (Zakaria et al., 2021).

Iodine adsorption plays a crucial role in the production of ACs, influencing their properties and applications. Iodine adsorption is integral to the characterization of ACs, with the iodine number being a widely recognized parameter for the rapid assessment of AC quality (Benadjemia et al., 2011). It represents the amount (in milligram) of iodine adsorbed per gram of the carbon at is surface, reflecting its porosity and adsorption capacity. This metric is known for its simplicity, as it provides a quick estimate of surface area and porosity, encapsulating the two-dimensional area of a carbon's surface and its pore size distribution (Stoycheva et al., 2023). Most high-quality ACs are characterized by iodine number equal to or exceeding 900 mg/g (Benadjemia et al., 2011). Studies on the adsorption of iodine from various solutions and vapor provide insights into the structural properties of ACs (Kurisingal et al., 2023; Zhao et al., 2023). Activated carbons are utilized in the recovery of iodine from dilute solutions, demonstrating their efficient adsorption capabilities (Bade et al., 2022). The iodine value of AC can vary based on the production method. Different chemical activations lead to diverse iodine values, influencing the suitability of AC for specific applications (Zhao et al., 2023).

Within the Leguminoseae family and the Mimosoideae subfamily, the African oil bean (*Pentaclethra macrophylla*) tree stands out, reaching approximately 6 meters in girth and 21 meters in height (Okpala, 2015). The seeds of this tree, enclosed in flat pods that burst upon maturation, are the most utilized part, leaving the pods as an underused waste product. Measuring about 35 to 45 cm in length and 5 to 10 cm in breadth, these black and woody pods have become a subject of interest due to their high fibre and fixed carbon contents (Okey-Onyesolu et al., 2018). There have been a few studies looking into the effects of preparation variables like temperature and impregnation ratio on activated carbons (ACs) from PM_{ps} (Abugu *et al*., 2015; Chimi *et al*., 2023), but very little is known in the literature about whether using a chemometric tool like Response Surface Methodology (RSM) to produce ACs from PM_{ps} could allow its structure to be developed further for enhanced adsorption performance. To address this gap, this study, therefore, focused on the optimal conditions for activating the untapped potential of PM_{ps} as precursor of ACs using potassium hydroxide (KOH) and phosphoric acid (H_3PO_4) as activating agents and iodine adsorption characterization approach. The study investigates how activation temperature, time, and impregnation ratio influence the iodine number of the ACs produced. Beyond optimizing the PM_p activation and carbonization, this study aims to provide valuable insights and reference points for utilizing this agroforestry waste material as a raw material for high-quality activated carbon production. The implications of this research extend to offering sustainable and economical solutions to water treatment, energy

Science World Journal Vol. 18(No 4) 2023 DOI: https://dx.doi.org/10.4314/swj.v18i4.22
www.scienceworldjournal.org
ISSN: 1597-6343 (Online), ISSN: 2756-391X (Print)
Published by Faculty of Science, Kaduna State University

storage, and CO_2 capture applications.

Experimental Procedures

Materials and Reagents

The PM_{ps} were obtained from the southern region of Benue State, Nigeria, where they are found in abundance during their peak dispersal periods from September to November. Preliminary assessments of the PM_{ps} collected were performed via proximate analysis using an electrical oven and furnace based on the American Society for Test and Materials (ASTM) standards E790, E830, and E897 (Zhang et al., 2022). In performing the proximate analysis, the moisture content of the PM_{ps} was determined at a temperature of 105°C, the ash content was determined within a temperature range from 105 to 550°C, the volatile matter content was determined at a temperature range from 105 up to 900°C, and the fixed carbon content was determined as the difference of the sum of percent moisture content, ash content, and volatile matter from 100%; it is assumed to be the carbon skeleton of the precursor at a temperature of 900°C and above. The ultimate analysis of the PM_{ps} was performed using LECO-CHNO-932 analyzer. The pods were cleaned to remove dirt and sun-dried for three (3) days to reduce their moisture contents. The biomaterials were transformed into granules using a combination of manual and mechanical size reduction mechanisms: cutting, pounding, and grinding. The PM_{ps} were passed through sieves of size 50 to 80 meshes (0.180 to 0.300 mm) to achieve experimental uniformity. They were stored in jute bags and labelled appropriately. Also, standard analytical grades of KOH, 85 wt% H_3PO_4, iodine, hydrochloric acid, and sodium thiosulphate were purchased from a retail chemical company at Makurdi and used without any further purification.

Synthesis of the Activated Carbon

The 85 wt% mass fractions of H_3PO_4 and 50 mg of the PM_{ps} granules were mixed according to the designed ratios of 1:1, 2:1, 3:1, 4:1, and 5:1 (ratios of the volume of H_3PO_4 to the mass of PM_{ps} granules) inside some sets of steel reactors that were agitated continuously at 1000 rpm on a centrifuge for 6 hours. The PM_{ps} were filtered out of the mixtures and the samples were dried using a thermostat oven set at 110°C for 1 hour to prepare the impregnated samples. The reactors were placed inside a high carbonization temperature tube furnace and heated from ambient temperature to 200°C for 30 minutes, followed by further heating at the different designed temperatures ranging from 200 to 700°C and activation time ranging from 20 to 210 minutes for simultaneous carbonization and activation of the precursors (Jiang *et al.*, 2019). The air within the furnace was displaced by introducing a nitrogen gas stream at 60 mL/min into it for 20 min.

Similar procedures were followed to produce ACs from the PM_{ps} granules using KOH powder. However, the chemical impregnation of the biomaterial was done by mixing the required mass of KOH and the PM_{ps} granules to attain the designed ratios inside separate steel reactors with 30 ml of deionized water (Jiang *et al*., 2019). After the samples were dried in a thermostat oven set at 110°C for 1 hour, they were transferred inside the furnace to be pyrolyzed at the different designed production conditions. All the carbonized chars were allowed to cool to room temperature and thereafter washed several times with 200 ml hot and cold distilled water to achieve a neutral pH, and then allowed to dry for 2 hours at 110°C using the oven. The activated carbons were boiled with HCl solution under reflux to remove impurities and to reduce their inherent ash contents. Figure 1 is the flowchart of the major steps involved in the PM_{ps} activated carbon production.

The products were pounded in a laboratory mortar and sieved using Tyler's sieves and stored in airtight containers. The dried carbon yield was determined using Eq. (1).

$$\text{Carbon Yield}, C_Y = (1 - m_c/m_r) \times 100 \quad (1)$$

where C_Y is the carbon yield (%), m_c is the mass of the carbonized product (g), and m_r is the mass of precursor (g).

Iodine Adsorption Studies

In this study, iodine served as the adsorbate of interest to evaluate the adsorptive performance of the PM_{ps} activated carbons (PMACs). Batch experimental studies were conducted in Erlenmeyer flasks, following the standard test method established by the ASTM D, (2006). To prepare the iodine stock solution, 2.70 g of iodine crystals and 4.10 g of potassium iodide (KI) were dissolved in 1 litre of deionized water. This solution was standardized using a standard solution of sodium thiosulphate (Pongener *et al*., 2015). Additionally, a starch solution, serving as the indicator reagent, was prepared by dissolving 0.30 g of starch powder in 30 ml of deionized water, to which 70 ml of boiled deionized water was added (Pongener *et al*., 2015). For each experimental run, 0.50 g of each category of PMACs and 10 ml of 5%v/v hydrochloric acid (HCl) were introduced into a 100 ml Erlenmeyer flask. The flask was gently stirred to wet the carbon, and then 100 ml of the iodine stock solution was added. The mixture was shaken on a shaker for 1 hour.

Science World Journal Vol. 18(No 4) 2023 DOI: https://dx.doi.org/10.4314/swj.v18i4.22
www.scienceworldjournal.org
ISSN: 1597-6343 (Online), ISSN: 2756-391X (Print)
Published by Faculty of Science, Kaduna State University

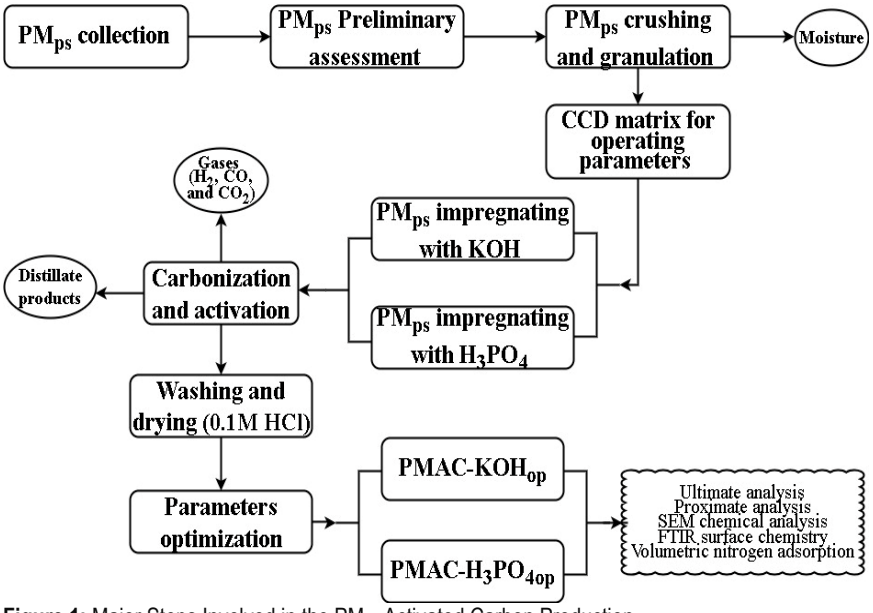

Figure 1: Major Steps Involved in the PM_{ps} Activated Carbon Production

Subsequently, the mixtures were filtered using microfiber filters, and a 20 ml aliquot portion of the filtrate was titrated with 0.10 M sodium thiosulphate. Additionally, 2 to 3 pipette drops of the starch solution were added as an indicator (Pongener *et al*., 2015). The mixture was stirred gently until it turned colourless. The initial and final volumes of the mixture, along with the titre value, were recorded for each experimental run. To establish a baseline, a blank titration procedure was performed using sodium thiosulphate solution without the addition of PMACs. This rigorous experimental protocol aimed to systematically evaluate the iodine adsorption efficiency of PMACs through meticulous titration and measurement procedures. The concentration of iodine adsorbed by the PMACs at room temperature was calculated using Eq. (2) (Bello et al., 2017).

$$I_n = [((A - B)/A) \times ((V \times M)/W)] \times 253.81 \quad 2$$

where I_n was the iodine number (mg/g), and A and B were the volumes of sodium thiosulphate solution required for blank and sample titrations, respectively. W is the mass of the PMACs sample, M is the molar concentration of iodine, V is the 20 ml aliquot, and 253.81 is the atomic mass of iodine.

The Central Composite Experimental Design for PMACs Production

The chemometric tool utilized for the study is Response Surface Methodology (RSM), a framework comprising various statistical and mathematical principles. RSM facilitates the quantitative analysis of data derived from designed experiments (Montgomery, 2017), enabling the determination of regression models and optimal operating conditions. Its utility extends to the development, improvement, and optimization of processes represented by the model. Notably, RSM excels in reducing and evaluating the number of experimental trials within full factorial experiments, including their interactions, without compromising expected outcomes (Iwar et al., 2022). In RSM, all independent variables are assumed to be continuous and controllable by the experiment with negligible error, while the response or dependent variable is considered a random variable (Montgomery, 2017). For this study, the chosen chemometric tool is the Central Composite Rotatable Design (CCD), which functions as a subset of RSM. The CCD configuration involves the following key components: (i) two-level factorial (2^3) – coded as -1 and +1, representing lower and higher levels; (ii) six replicates located at the center (0, 0, 0) to assess experimental error and data reproducibility, and (iii) six axial points located at (±α, 0, 0), (0, ±α, 0), and (0, 0, ±α), where α represents the distance of an axial point from the center (α = 1.68). These points render the design rotatable. The incorporation of these components results in a total of 20 experimental runs. The CCD design is particularly advantageous for efficiently exploring the experimental space, considering factorial combinations, and assessing the impact of variables on the response within a reasonable number of trials (Ogbeh & Ominiyi, 2022).

The PMACs were prepared using three independent parameters namely the activation temperature (A), activation time (B), and impregnation ratio (C). The coded and real levels of these parameters are shown in Table 1. The responses of the design were the iodine number and the carbon yield. The attributes of the experimental responses were predicted from the second-order polynomial regression model generally described as Eq. (3) (Genli et al., 2022).

$$Y_{I_n \text{ or } C_Y} = \beta_o + \sum_{i=1}^{n} \beta_{ii} X_i + \left(\sum_{i=1}^{n} \beta_{ii} X_i \right)^2 + \sum_{i=1}^{n-1} \sum_{j=i+1}^{n} \beta_{ij} X_i X_j \quad 3$$

where Y is the predicted response, β_o is the constant coefficient, β_i represents the linear term coefficients, β_{ij} represents the interaction coefficients, β_{ii} represents the quadratic coefficients, X_i, X_j are the coded values of the production parameters and n is the number of variables. The experimental sequence was randomized to minimize the effects of the uncontrolled factors and outliers. The significance of each coefficient in the models was determined by F-test and *p*-values. The CCD of the RSM and its corresponding

Science World Journal Vol. 18(No 4) 2023 DOI: https://dx.doi.org/10.4314/swj.v18i4.22
www.scienceworldjournal.org
ISSN: 1597-6343 (Online), ISSN: 2756-391X (Print)
Published by Faculty of Science, Kaduna State University

statistical analyses were done using Design-Expert (version 10.0 Stat-Ease Inc., Minneapolis, MN).

Characterization of the Activated Carbons

For each of the activated carbons (PMACs) produced using the two activating agents (KOH and H_3PO_4) at the optimum operating conditions determined statistically using the Design Expert Software, the organic structure properties were determined using a Thermo Nicolet Fourier transform infrared spectrometer (Nicolet 67, USA).

Table 1: Coded and Actual Levels of Production Parameters Used to Produce the PMACs.

Production factor	Coded levels				
	-α (-1.68)	-1	0	+1	+α (+1.68)
	Actual values				
Activating temperature (°C), A	200	300	450	600	700
Activating time (min), B	20	60	120	180	210
Impregnation ratio (g/L), C	1	2	3	4	5

The textural parameters and elemental constituents of the activated carbons were determined using scanning electron microscopy combined with energy-dispersive X-ray spectroscopy (EDX). Volumetric adsorption analyzer (Micrometrics 3Flex version 5.02) was used to determine the specific surface area through nitrogen adsorption Brunauer-Emmett-Teller (BET) equation. The total pore volume (V_t) and the average pore diameter of the activated carbons were determined as the liquid volume of nitrogen (N_2) adsorption at a relative pressure (P/P_o) of 0.99 (Ahmad & Alrozi, 2011).

RESULTS AND DISCUSSION

Yields of the *Pentaclethra macrophylla* Activated Carbons

The experimental design matrix used to prepare the PMACs with both activating agents (KOH and H_3PO_4) is shown in Table 2. Even though the yields of the PMACs prepared with both activating agents were moderately high, the PMACs yields from using the same quantity of the PM_{ps} with the activating agents differ from one another, with PMACs obtained from using the H_3PO_4 activating agent demonstrating higher yields than those obtained from using the KOH activating agent. Generally, increasing the impregnation ratio, especially with activating agents like KOH or H_3PO_4, results in a gradual decrease in the yield of activated carbon (Zakaria et al., 2021). However, increasing impregnation ratio involving H_3PO_4 activating agent leads to an increase in burning rate and porosity, contributing to a rise in surface area (Zięzio et al., 2020). The reasons for the relatively lower activated carbon yields from using the KOH activating agent is unclear. However, it may be attributed to the tendency of KOH to promote intense volatilization of biomass through the breaking of C-O-C and C-C bonds (Yokoyama et al., 2019). Furthermore, pyrolysis involving the use of KOH as an activating agent has been reported to favour catalytic decomposition of heteroatoms within biomass, which promotes the increased release of gases like CO, CO_2, water vapour, and hydrocarbons (Jamnongkan et al., 2022).

Experimental Data and Model Building

Polynomial regression models were developed using the CCD to analyse the correlation between the parameters used to produce the activated carbons, with respect to their iodine number and carbon yield. The effects of the independent factors and their interactions on each of the responses were analysed and optimized to investigate the PMAC with higher adsorption performance. The results indicate that the three independent parameters (activation temperature, activation time, and impregnation ratio) and their respective ranges were similar in the design used to produce the PMACs.

Science World Journal Vol. 18(No 4) 2023 DOI: https://dx.doi.org/10.4314/swj.v18i4.22
www.scienceworldjournal.org
ISSN: 1597-6343 (Online), ISSN: 2756-391X (Print)
Published by Faculty of Science, Kaduna State University

Table 2: The CCD Experimental Matrix both Iodine Numbers and Carbons Yield

Run	A (°C)	B (min)	C (ml/g)	Iodine number, I_n (mg/g)		Carbon yield, C_y (%)	
	value & code	value & code	value & code	$PMAC_{KOH}$ observed	$PMAC_{H3PO4}$ observed	$PMAC_{KOH}$ observed	$PMAC_{H3PO4}$ observed
1	450 (0)	120 (0)	3 (0)	911.43	642.00	39.98	48.86
2	300 (-1)	60 (-1)	4 (+1)	674.17	393.61	47.21	56.31
3	450 (0)	120 (0)	3 (0)	911.43	632.00	39.40	46.97
4	600 (+1)	180 (+1)	2 (-1)	955.20	769.93	31.30	40.06
5	600 (+1)	60 (0)	4 (+1)	1026.42	531.60	31.89	41.5
6	300 (-1)	180 (+1)	4 (+1)	720.54	427.77	40.81	50.59
7	300 (-1)	180 (+1)	2 (-1)	861.11	292.00	40.97	51.02
8	600 (+1)	60 (-1)	2 (-1)	653.72	683.30	32.05	40.66
9	300 (-1)	60 (-1)	2 (-1)	466.57	434.01	44.78	51.33
10	450 (0)	120 (0)	3 (0)	950.38	658.00	39.33	48.41
11	450 (0)	120 (0)	3 (0)	911.43	668.00	39.33	48.51
12	600 (+1)	180 (+1)	4 (+1)	991.96	810.06	29.43	36.37
13	450 (0)	120 (0)	3 (0)	911.43	658.00	39.45	48.56
14	450 (0)	20 (-1.68)	3 (0)	794.51	591.20	39.65	46.65
15	450 (0)	120 (0)	1 (-1.68)	454.74	633.79	37.72	48.76
16	700 (+1.68)	120 (0)	3 (0)	1011.64	743.68	30.35	38.45
17	450 (0)	120 (0)	3 (0)	911.43	668.00	39.30	49.01
18	200 (-1.68)	120 (0)	3 (0)	651.34	217.37	50.44	60
19	450 (0)	120 (0)	5 (+1.68)	688.89	629.67	37.86	49.56
20	450 (0)	210 (+1.68)	3 (0)	1050.60	681.08	34.99	43.27

However, the results of the analysis indicate that their effects on the responses were different. This outcome specify that any activated carbons derived from different precursors might have different characteristics, even though the same conditions were administered to produce them (Ahmad et al., 2020). The distinct variations of the I_n values, ranging from 454.74 to 1050.60 mg/g and C_Y values, ranging from 29.34 to 51.30% for the PMAC-KOH and the I_n values, ranging from 217.37 to 810.06 mg/g and C_Y values, ranging from 38.45 to 60.0% for PMAC-H_3PO_4 are at the instant of the variations of each of these independent operating parameters. The effects of the variation of these parameters on the I_n and C_y are shown in the ANOVA Tables 3 and 4 for PMAC-KOH and PMAC-H_3PO_4, respectively. Further analysis of data using the Software for both responses (I_n and C_Y) consistently recommended selecting quadratic models. During the model selection process, the sequential model sum of squares guided the choice, favouring the highest-order polynomials. This decision was influenced by the identification of additional terms deemed statistically significant ($p \leq 0.5$), ensuring that the selected models were not aliased. The ultimate outcome is represented by the final empirical models in the coded factors form, as Eqns 4 to 7 for prediction of iodine adsorption (iodine number) and carbon yield of PMAC-KOH and PMAC-H_3PO_4, respectively. Each of the operating parameters created both synergetic (positive coefficients) and antagonistic (negative coefficients) effects on the I_n and C_y values of both activated carbons, as indicated in the statistical regression models. However, any parameter found to be non-significant at $p \geq 0.05$ on the ANOVA table was removed from each of the models. With regards to I_n, it was discovered that only the interaction of activation time and impregnation ratio (BC) for the PMAC-H_3PO_4 was not significant. With respect to the effects of the operating parameters on carbon yield, however, the effects of the activating agents and even the varying impregnation ratios were discovered to be minimum and negligible, and this is confirmed by the non-significance of C and BC in the regression model for the PMAC-KOH (Eq. 6) and C and AC in the (Eq. 7) for PMAC-H_3PO_4.

$$I_{KOH} = -1108.06 + 1.52A + 6.66B + 629.66C - 2.42 \times 10^{-3}AB + 0.29AC - 1.43BC - 1.50A^2 - 88.00C^2 \quad (4)$$

$$I_{H_3PO_4} = -274.56 + 3.62A - 3.71B + 6.57 \times 10^{-3}AB - 0.17AC + 0.77BC - 3.17 \times 10^{-3}A^2 - 4.38 \times 10^{-3}B^2 - 11.35C^2 \quad (5)$$

$$C_{KOH} = 48.72 - 0.04A + 0.04B + 9.72 \times 10^{-5}AB - 3.58 \times 10^{-3}AC - 8.96 \times 10^{-3}BC - 3.38 \times 10^{-4}B^2 - 0.590C^2 \quad (6)$$

$$C_{H_3PO_4} = 46.42 - 0.02A + 0.16B - 6.17 \times 10^{-3}AC - 0.02B - 5.02 \times 10^{-4}B^2 \quad (7)$$

Regarding the models for the iodine numbers of PMAC-KOH and PMAC-H_3PO_4 (Eqs 4 and 5, respectively), several key observations can be made. Positive linear coefficients were evident for all three parameters contributing to the development of high iodine number in PMAC-KOH (Eq. 4). Notably, the contribution from the impregnation ratio (+629.66) was particularly significant, especially considering its lack of significance in the production of the PMAC-H_3PO_4 (Eq 5). While both the activation temperature and impregnation ratio exhibited positive linear effects on the preparation of both PMAC-KOH and PMAC-H_3PO_4, the interactions (AB) between these parameters showed reverse coefficients.

Science World Journal Vol. 18(No 4) 2023 DOI: https://dx.doi.org/10.4314/swj.v18i4.22
www.scienceworldjournal.org
ISSN: 1597-6343 (Online), ISSN: 2756-391X (Print)
Published by Faculty of Science, Kaduna State University

Negative coefficients of interaction between temperature and impregnation ratio (AC) were crucial for impacting the iodine number of PMAC-KOH, while positive coefficients were influential for PMAC-H_3PO_4. This suggests that a higher temperature may be required for the simultaneous dehydration and carbonization of KOH-impregnated PMps,

Table 3: Results of ANOVA for Iodine Number (mg/g) of the PMACs

Source		I_n (Iodine number (mg/g))							
	df	SS_K	SS_H	MS_K	MS_H	F_K	F_H	P_K	P_H
Model	9	598381.46	466637.83	66486.83	51848.65	327.60	302.04	0.00	4E-10
A-act. Temp.	1	167183.06	333020.60	167183.06	333020.60	823.76	1939.97	0.00	8E-12
B-act. Time	1	94734.59	11345.52	94734.59	11345.52	466.79	66.09	0.00	2E-05
C-impreg. Ratio	1	55789.26	37.33	55789.26	37.33	274.89	0.22	0.00	7E-01
AB	1	3779.72	27959.03	3779.72	27959.03	18.62	162.87	0.00	5E-07
AC	1	14657.29	5353.02	14657.29	5353.02	72.22	31.18	0.00	3E-04
BC	1	58500.81	16928.00	58500.81	16928.00	288.25	98.61	0.00	4E-06
A^2	1	15661.11	70225.26	15661.11	70225.26	77.17	409.09	0.00	8E-09
B^2	1	48.43	2958.79	48.43	2958.79	0.24	17.24	0.64	2E-03
C^2	1	197921.06	3297.18	197921.06	3297.18	975.22	19.21	0.00	2E-03
Residual	9	1826.55	1544.96	202.95	171.66				
Lack of fit	5	688.73	718.96	137.75	143.79	0.48	0.70	0.78	7E-01

Table 4: Results of ANOVA for yield (%) of the PMACs

Source		C_y (Carbon yield)							
	df	SS_K	SS_H	MS_K	MS_H	F_K	F_H	P_K	P_H
Model	9	570.73	633.45	63.41	70.38	278.34	202.65	0.00	3E-09
A-act. Temp.	1	503.12	552.95	503.12	552.95	2208.32	1592.07	0.00	2E-11
B-act. Time	1	36.43	26.53	36.43	26.53	159.92	76.40	0.00	1E-05
C-impreg. Ratio	1	0.02	0.68	0.02	0.68	0.07	1.96	0.79	2E-01
AB	1	6.13	0.01	6.13	0.01	26.88	0.03	0.00	9E-01
AC	1	2.31	6.84	2.31	6.84	10.14	19.71	0.01	2E-03
BC	1	2.31	12.35	2.31	12.35	10.14	35.56	0.01	2E-04
A^2	1	0.06	0.03	0.06	0.03	0.25	0.10	0.63	8E-01
B^2	1	17.64	38.92	17.64	38.92	77.42	112.07	0.00	2E-06
C^2	1	8.89	0.04	8.89	0.04	39.04	0.11	0.00	7E-01
Residual	9	2.05	3.13	0.23	0.35				
Lack of fit	5	1.74	0.94	0.35	0.19	4.51	0.34	0.08	9E-01

Legend: SS_K and SS_H are the sum of square, MS_K and MS_H are the mean square, F_K and F_H are the F-calculated, and P_K and P_H are the P-values obtained from analysing the $PMAC_{KOH}$ and PM_{H3PO4} iodine numbers and carbon yields, respectively.

Science World Journal Vol. 18(No 4) 2023 DOI: https://dx.doi.org/10.4314/swj.v18i4.22
www.scienceworldjournal.org
ISSN: 1597-6343 (Online), ISSN: 2756-391X (Print)
Published by Faculty of Science, Kaduna State University

while a slightly lower temperature may be needed for the development of H_3PO_4-impregnated PMps. The yields of both are influenced by activation temperature and time, with impregnation ratio playing a lesser role (as indicated by Eqs 6 and 7). Positive coefficients of interactions between temperature and time (AB) were essential for impacting the yields of both KOH-PMACs and H_3PO_4-PMACs. However, the reverse was observed for all other interactions involving the impregnation ratio and the other two parameters (temperature and time), respectively. Figures 2a and 2c and the models Eqs 4 and 6 indicated high coefficients of determination (R^2 = 0.9969 and 0.9964) and low standard deviations (SD = 14.25 mg/g and 0.48%) for the iodine number and carbon yield of the PMAC-KOH, respectively. The adjusted R^2 values for the iodine number and yield of PMAC-KOH were 0.9968 and 0.9962, respectively. The strong agreement between the actual experimental and predicted data for the models suggested in Eqs. 4 and 6, underscores the models' suitability and competence in predicting the experimental responses (I_n and C_y). Similarly, for the PMAC-H_3PO_4, high coefficients of determination (R^2 = 0.9967 and 0.9952) and low standard deviations (SD = 13.10 mg/g and 0.59%) were obtained for the regression models (Eqs 5 and 7), representing the iodine number (I_n) and carbon yield (C_y) (Figures 2b and 2d), respectively. The adjusted R^2 values for the iodine number and yield of PMAC-H_3PO_4 were 0.9965 and 0.9948, respectively. The strong agreement between the actual experimental and predicted data for the models suggested in Eqs. 5 and 7, further affirm the suitability and competency of the models in accurately predicting the experimental responses.

activated carbons were signific

Profile of Iodine Adsorption by the Activated Carbons

Examining the F values (F_K and F_H) corresponding to each of the independent factors (A, B, and C) for PMAC-KOH and PMAC-H_3PO_4 in Table 3 reveals significant and substantial effects on iodine adsorption (iodine number) onto both PMACs. Although all factors exhibit considerable impacts, their degrees of influence on the iodine number of the PMACs differ from one another. Through comparative analysis, it is evident that activation temperature (factor-A) exerts a more significant effect on iodine adsorption onto PMAC-H_3PO_4 than onto PMAC-KOH. Conversely, both activation time (factor-B) and impregnation ratio (factor-C) display higher significant effects on iodine adsorption for PMAC-KOH and PMAC-H_3PO_4. However, their effects on PMAC-KOH are notably greater than on PMAC-H_3PO_4. Among all considered factors, activation temperature holds the greatest influence on iodine adsorption, as indicated by its highest F-values. The interactive effects (AB, AC, and BC) between the parameters on the iodine number were all significant for PMAC-KOH but only (AB and AC) were significant for PMAC-H_3PO_4. However, the interaction between activation time (factor-B) and impregnation ratio (factor-C) being notably higher than other interaction categories.

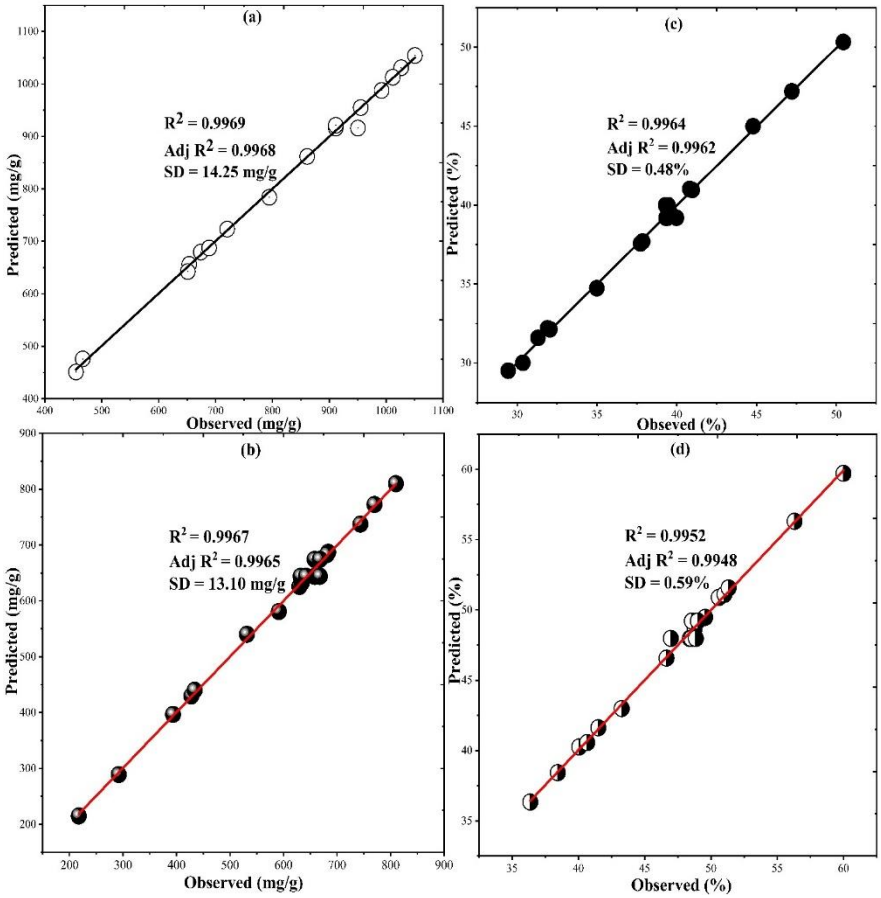

Figure 2: Predicted versus actual values of Iodine Numbers (a and b) and Yields (c and d) for PMAC-KOH and PMAC-H_3PO_4, respectively.

Science World Journal Vol. 18(No 4) 2023 DOI: https://dx.doi.org/10.4314/swj.v18i4.22
www.scienceworldjournal.org
ISSN: 1597-6343 (Online), ISSN: 2756-391X (Print)
Published by Faculty of Science, Kaduna State University

Figure 3 illustrates the influence of activation temperature and activation time (AB), activation temperature and impregnation ratio (AC), and activation time and impregnation ratio (BC) on the iodine numbers of PMAC-KOH and PMAC-H_3PO_4. The effectiveness of iodine adsorption by both PMAC-KOH and PMAC-H_3PO_4 is minimal at the lowest impregnation ratio, moderate activation temperature, and activation time, as confirmed by the data in Table 2 (run number 15). With increasing values of these variables, iodine adsorption efficiencies for both PMAC-KOH and PMAC-H_3PO_4 also increase, reflected in the iodine numbers. However, PMAC-KOH becomes increasingly ineffective in adsorbing additional iodine when extreme conditions like high temperature, moderate activation time, and extremely low impregnation ratio are employed. In contrast, PMAC-H_3PO_4 reaches a point of ineffectiveness when using conditions such as low activation temperature, moderate activation time, and low impregnation ratio.

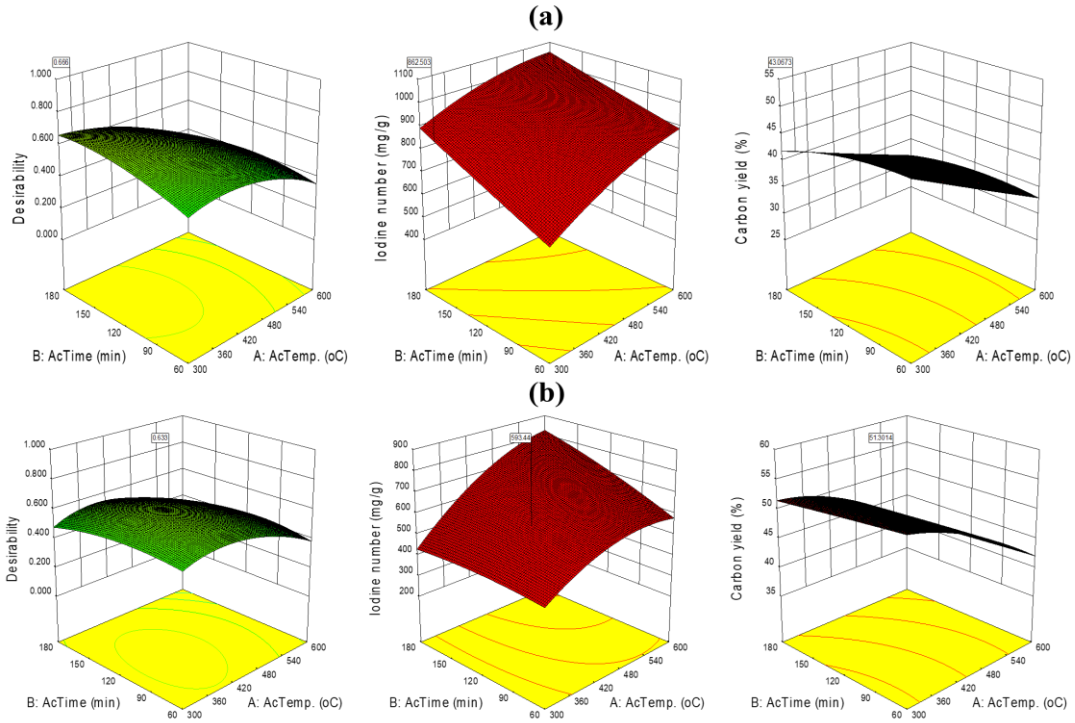

Figure 3: 3D Graphical Plots of the Effects of the optimum production parameters on both responses (iodine number and Carbon yields) of (a) PMAC-KOH and (b) PMAC-H_3PO_4

This observation aligns with previous studies, where excessively high activation temperatures result in blocked pores due to excess carbonization (Gao et al., 2020), and too low impregnation ratios render the chemical activation process less effective (Zakaria et al., 2021), resulting in fewer developed pores. Additionally, activation temperatures above 500 °C are believed to significantly impact the carbon material, causing drastic expansion, creating larger surface areas, and inducing high porosity through the intercalation of metallic potassium hydroxide (Wang et al., 2019). The relatively high iodine adsorption capacities of the activated carbons produced might be useful for removal of radioactive isotopes of iodine that are often released from uranium power plant (Kurisingal et al., 2023).

Operating Parameters Optimization and Validation

The primary objective of the experimental design is to identify the optimal process parameters that result in high iodine numbers and yields for both PMAC-KOH and PMAC-H_3PO_4. However, optimizing these responses concurrently poses a challenge because they represent different regions of interest. For instance, increasing iodine adsorption performance tends to decrease the yield of activated carbons, and vice versa. Therefore, the identification of two sets of optimum process conditions is necessary. Table 5 provides the model validation results for PMAC-KOH and PMAC-H_3PO_4, with the selected optimized parameters experimentally verified. The optimization process utilized the same software to set the target criteria at the maximum value, while the variable values were constrained within the studied range. The adsorbents were prepared under optimal conditions, with the factors (activation temperature, activation time, and impregnation ratio) set within the design range, and the responses (iodine number and carbon yield) set to the highest value. The resulting optimized PMACs were labelled PMAC-KOH_{op} and PMAC-H_3PO_{4op}. For the preparation of PMAC-KOH_{op}, the optimal operating parameters were determined as follows: the activation temperature of 450°C, activation time of 120 min, and impregnation ratio of 3. This configuration led to an iodine adsorption of 918.58 mg/g and a PMAC-KOH yield of 39.60%. Similarly, for the preparation of PMAC-H_3PO_{4op}, the optimal parameters were activation temperature of 400°C, activation time of 112.45 min, and impregnation ratio of 3.73. This resulted in an iodine adsorption of 593.44 mg/g and a PMAC-H_3PO_{4op} yield of 51.30%. The experimental values obtained at these optimum preparation conditions closely aligned with the predicted values from the models. However, small negative

Science World Journal Vol. 18(No 4) 2023 DOI: https://dx.doi.org/10.4314/swj.v18i4.22
www.scienceworldjournal.org
ISSN: 1597-6343 (Online), ISSN: 2756-391X (Print)
Published by Faculty of Science, Kaduna State University

percentage errors between the actual and predicted values were recorded for both sets of activated carbons. This discrepancy is minor and further validates the suitability of the model in affirming its sufficiency for predicting the responses. In comparison with the ideal iodine numbers of commercial granular activated carbons (GACs) used for pollutant removal from wastewater, only the PMAC-KOH_{op} fall within the typical range of 800 to 1200 mg/g (Cendekia et al., 2021). Since any GAC with higher iodine numbers generally exhibit greater adsorption efficiency and are considered more effective for the removal of pollutants in wastewater treatment processes, the PMAC-KOH_{op} could perform well as a pollutant adsorbent.

Table 5: Model Validation and Optimum production parameters for Responses (I_n and C_Y)

Activated carbon	A (oC)	B (min)	C	I_n (mg/g) Predicted	I_n (mg/g) Observed	Error (%)	C_y (%) Predicted	C_y(%) Observed	Error (%)
PMAC-KOH_{op}	450	120	3	918.58	916.56	-0.22	39.60	39.15	-1.15
PMAC-H_3PO_{4op}	400	112.45	3.73	593.44	592.88	-0.09	51.30	51.1	-0.39

Proximate and Ultimate Analysis

The results of the proximate and ultimate analysis of the PM_{ps} and the activated carbons are shown in Table 6. The proximate and elemental analyses were necessary to understand the potential properties of activated carbons, which is essential for controlling their properties and potential functions. The relatively high moisture content (19.14%) of the PM_{ps} is an indication that high energy might be expended to dry up any excess moisture during the production process. Besides, excess moisture in biomass tend to affect the porosity of the resulting activated carbon, as excess moisture regulate the movement of the activating agent during the activation process (Zieliński et al., 2022).

Table 6: Proximate and ultimate analyses of *PM* pods and the Activated Carbons

Sample	Proximate analysis (wt% ar[a])				Ultimate analysis (wt% ar[a])				
	Moisture	Volatile matter	Fixed carbon	Ash	C	H	N	O[b]	S
PM_{ps}	19.14	54.31	23.37	3.88	45.47	31.89	3.14	17.54	1.96
PMAC-KOH	3.12	15.83	78.48	2.57	82.64	11.22	1.05	4.11	0.98
PMAC-H_3PO_4	7.02	18.68	70.58	3.72	72.31	18.06	2.96	5.56	1.11

[a] on wet basis as received; [b] calculated by difference

The proportion of fixed carbon also affects the structure and porosity of activated carbons. Higher fixed carbon yields activated carbons of stronger structural stability (Montoya-Suarez et al., 2016). The amount of ash in biomass affects the purity of the activated carbon, which can hinder activation. Higher porosity is necessary for high-grade activated carbon, which is difficult to adsorb. Lower ash content is necessary for improved adsorption quality. The $PM_{ps,}$ just like most biomass, consists of various elements such as carbon, hydrogen, nitrogen, sulphur, and oxygen. As the carbon content increases, so does their quality and ability to act as an adsorbent. In addition to the fixed carbon content, higher carbon content of the precursor generates activated carbons of better adsorption capability (Montoya-Suarez et al., 2016). The activation of functional groups is driven by various elements, and only when individual elements are controlled to a certain level that activated carbons with specific surface chemistries can be prepared (Amin et al., 2023). Controlling individual elements to a certain level can result in different levels of adsorption selectivity, allowing for the development of activated carbons with specific surface chemistries.

Surface Morphologies of the Activated Carbons

Further characterization of activated carbons prepared with the optimum operating parameters was performed. In general, the chemical activation of the PMps with KOH and H_3PO_4 revealed notable variations in the textural structure of the material before and after the activation processes. SEM micrographs of the PMps, as shown in Figure 4a, reveal the raw material's curly surface lacks pores and cavities. The carbonization and activation processes induced development of few pores from initially occupied sites by volatile matter and moisture. Activated carbons exhibit early-stage small pores, possibly due to residues of tarry substances from calcination. Enhanced interaction between KOH and the carbon, at elevated activation temperature, results in well-developed pores. The SEM image of PMAC-KOH_{op} Figure 4b confirms multiple pores, affirming the effectiveness of KOH chemical activation. This is consistent with (Baba et al., 2023), carbonization products exhibit increased surface porosity, evidenced by small voids. The H_3PO_4 activation on PMAC-H_3PO_{4op} surface, shown in Figure 4c, creates more pores, attributed to H_3PO_4 diffusion favouring increased H_3PO_4-carbon reaction via acid hydrolysis. The diverse surface porosity suggests potential varied applications for the synthesized activated carbons. This suggests that the structure of PMAC-KOH_{op} contained a higher ratio of porous structures than in the PMAC-H_3PO_{4op}. The higher iodine numbers obtained for PMAC-KOH_{op} indicates the availability of more porous structures within the activated carbon, demonstrating a greater affinity for the adsorption of small molecules (Karim et al., 2022).

Science World Journal Vol. 18(No 4) 2023 DOI: https://dx.doi.org/10.4314/swj.v18i4.22
www.scienceworldjournal.org
ISSN: 1597-6343 (Online), ISSN: 2756-391X (Print)
Published by Faculty of Science, Kaduna State University

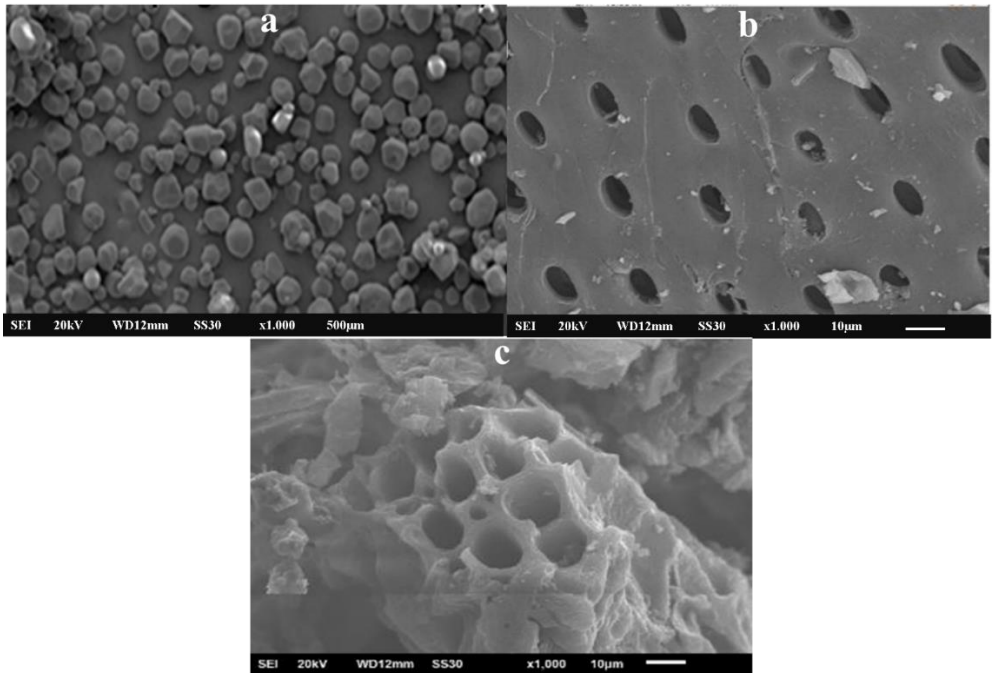

Figure 4: Scanning Electron Micrographs of the (a) PM_{ps} (b) PMAC-KOH_{op} (c) PMAC-H_3PO_{4op} Functional Groups in the Precursor and the Activated Carbons

The extent of modification of the porous structure of the PMps and the activated carbons derived from them using KOH and H_3PO_4 activating agents is shown in Figures 5a, 5b, and 5c, respectively. The FTIR analysis of the PM_{ps} spectrum (Figure 4a) reveals peaks at 3640–3550 cm^{-1}, indicating antisymmetric O-H stretching vibration and C=H asymmetric stretching vibration bonds at 2936 cm^{-1} (Dai et al., 2023; Sarma et al., 2015). The peak at1766 cm^{-1} urea in various samples (Onija et al., 2012). The peak at 1424 cm^{-1} in the FTIR spectra of the PM_{ps} signifies aliphatic C-H bending vibration (Kalembkiewicz et al., 2018). This suggests the presence of aliphatic hydrocarbons or organic compounds in the PM_{ps}, indicating the composition of various biomolecules. The peak at 1308 cm^{-1} is associated with creatine (Jerônimo et al., 2012). In biomaterials containing creatine, this peak represents a specific

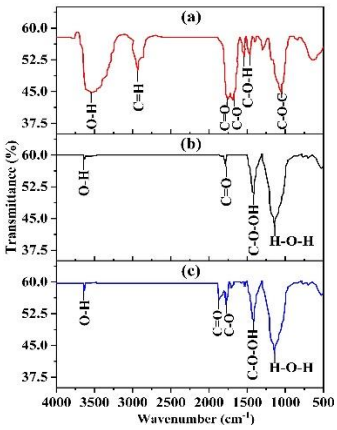

Figure 5: FT-IR Spectra of the (a) PMps, (b) PMAC-KOH_{op}, and (b) PMAC-H_3PO_{4op}

in the FTIR spectra is an intense band indicating the presence of C=O stretching vibration. This suggests the involvement of carbonyl groups, possibly from ketones or aldehydes within the PM_{ps} structure (Onija et al., 2012) and the peat at 1673 cm^{-1} correspond to aromatic skeleton (ν(C=O) + δ(N-H)) vibrations; it is a distinctive feature used for identifying

vibrational mode, aiding in the identification of creatine within the sample. The spectra may include carbonyl, alcohol, and cellulose groups. The differences between the PMAC-KOH_{op} and PMAC-H_3PO_{4op} spectra from PMps are mostly due to lost bands during activation and carbonization, which depend on the activation temperature.

Science World Journal Vol. 18(No 4) 2023 DOI: https://dx.doi.org/10.4314/swj.v18i4.22
www.scienceworldjournal.org
ISSN: 1597-6343 (Online), ISSN: 2756-391X (Print)
Published by Faculty of Science, Kaduna State University

The absence of peaks at 3600 cm^{-1} in both activated carbon spectra indicates decomposition of oxygenated hydrocarbons in cellulose and hemicellulose (Kurian et al., 2015). The decrease in intensity of the FTIR spectra of the PM_{ps} at 1240 cm^{-1} band suggests the destruction of the lignin structure often associated with specific vibrational modes relating to functional groups such as C-O and C-O-C in hemicellulose. A decrease in intensity at this wavenumber suggests a reduction in the concentration or structural changes of these groups within the PMps. The presence of additional functional groups in PMAC spectra indicates enhanced surface porosity, which contributes to improved efficiency of the PMAC adsorbent in trapping iodine molecules.

Structural and Porous Properties of the Activated Carbons

With reference to other prior studies, Table 7 shows the BET specific surface areas (SSA), total pore volume (V_t), and average pore diameter of the precursor and the activated carbons produced. The PM_{ps} initially exhibited a notably low BET SSA of 3.09 m^2/g. However, under the optimal operating conditions, the resulting PMACs, specifically PMAC-KOH_{op} and PMAC-H_3PO_{4op}, demonstrated substantial increases in the SSA, reaching 911.70 and 527.59 m^2/g, respectively. Faith et al., (2017) reported an iodine number of 764.53 mg/g and a surface area of 954.56 m^2/g for an activated carbon produced from *Pentaclethra macrophylla* (PM) seed shells with H_3PO_4 as activating agent. Both values are quite higher than the corresponding equivalent values of 592.88 mg/g and 527.59 m^2/g observed for the PMAC-H_3PO_{4op} in this study. The substantial difference between these values may be due to the inherent differences between the PM seeds shell and its pods. However, the enhancements observed in the structural and porous properties of both PMACs signify the effectiveness of the simultaneous chemical activation and carbonization of the PM_{ps} at the applied operating conditions. Throughout the activation and carbonization processes, volatile matter and water were systematically removed from the PM_{ps} through evaporation and dehydration. The optimum operating conditions influenced the severity of these processes, impacting the removal of these constituents from the precursor. The BET SSA of PMAC-KOH_{op} was quite higher than that of PMAC-H_3PO_{4op}, and this result aligned with other prior studies on activated carbons produced from agroforestry wastes using KOH and H_3PO_4 as activating agents (Van & Thu, 2019).

The total pore volumes recorded for the PMAC-KOH_{op} and PMAC-H_3PO_{4op} were 1.24 and 1.09 cm^3/g, respectively, with average pore diameters of 5.54 and 5.98 nm (Figures 6b and 6d). Additionally, the optimal conditions led to diverse development of vacant spaces and pores within the resulting ACs. In general, the porosity of the both PMAC-KOH_{op} and PMAC-H_3PO_{4op} increased with increase in all the operating parameters (temperature, time, and impregnation ratio). However, this does correspond with the resulting iodine number of each AC. This observation aligns with Chimi et al., (2023) report for the production of ACs from PMps with H_3PO_4 as activator. Moreover, despite potential variations of the influence of the different operating conditions, both sets of conditions exclusively yielded ACs that have average pore diameters all within the mesopore regions. Notably, the slightly lower average pore diameter of 5.54 nm in the PMAC-KOH_{op} could be attributed to the formation of potassium ions (e.g., K_2CO_3) with simultaneous emissions of CO_2 and CO during the KOH chemical activation (Thongpat et al., 2021). These ions, recognized for their high mobility, deeply penetrate the vacant spaces in the precursor and its char during the activation process for enhanced pore formation and increased surface area (Ahmad et al., 2020)

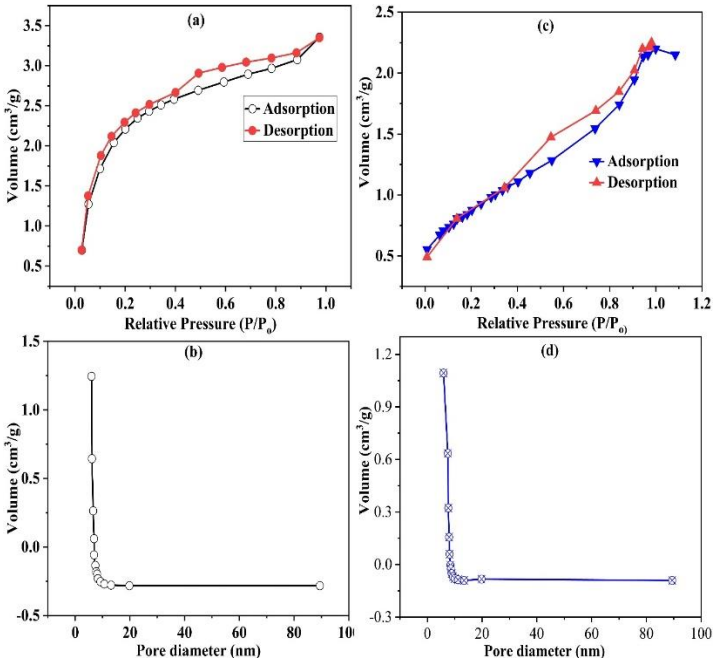

Figure 6: N_2 Adsorption-desorption Profiles (a and c) and Pore Properties (b and d) of PMAC-KOH_{op} and PMAC-H_3PO_{4op}, respectively.

Table 7: Comparison of the Surface Area and Pore Properties of the Activated Carbons with Other Studies

Sample	Activating agent	BET SA (m^2/g)	Pore volume (cm^3/g)			Pore diameter (nm)	Iodine number (mg/g)	Reference
			V_{tot}	V_{mic}	V_{mes}			
PM_{ps}	-	3.09	-	-	-	-	-	This present study
PMAC	KOH	911.70	1.24	-	-	5.54	916.56	This present study
PMAC	H_3PO_4	527.59	1.09	-	-	5.98	592.88	This present study
PMAC	H_3PO_4	-	-	-	-	-	955.31	(Chimi et al., 2023)
PMAC	H_2SO_4	954.56	-	-	-		764.53	(Okey-Onyesolu et al., 2018)
Coffee husk	KOH	520.55	-	-	-	-	603.45	(Ngueabouo et al., 2022)
Coffee husk	H_3PO_4	560.65	-	-	-	-	520.65	(Ngueabouo et al., 2022
Rubberwood chips	KOH	1491.75	0.678	0.581	-	1.82	-	(Thongpat et al., 2021)
Corncob	H_3PO_4	700.00	-	0.011	-	-	632.00	(El-sayed et al., 2014)
Sugar beet bagasse	H_3PO_4	748.00	0.36	-	-	1.19	1275.00	(Ghorbani et al., 2020)
Jujube stones	H_3PO_4	948.84	0.85	-	-	-	867.54	(Bouchelkia et al., 2023)

Conclusion

In this study, Response Surface Methodology (RSM) served as a chemometric tool for synthesizing activated carbons from Pentaclethra macrophylla pods (PMps), utilizing KOH and H_3PO_4 as activation agents. Optimal conditions were determined through numerical optimization, revealing that KOH activation at an impregnation ratio of 3:1, temperature of 450°C, and activation time of 120 minutes resulted in the highest predicted iodine number (918.58 mg/g) and carbon yield (39.60%), with observed values at 916.56 mg/g and 39.15%. Similarly, H_3PO_4 activation at an impregnation ratio of 3.7:1, temperature of 400°C, and activation time of 112 minutes achieved the highest predicted iodine number (593.44 mg/g) and carbon yield (51.30%). The observed values closely matched the predictions (592.88 mg/g and 51.10%). The PMAC-KOH_{op} and PMAC-H_3PO_{4op} exhibited specific surface areas, total pore volumes, and average pore diameters of 911.70 and 527.59 m^2/g, 1.24 and 1.09 cm^3/g, and 5.54 and 5.98 nm, respectively, indicating extensive graphitic features. FTIR spectra suggested higher aromaticity in PMAC-KOHop, implying enhanced electrostatic and π-π interactions. Future research should explore the adsorptive capabilities of these activated carbons in water treatment, addressing organic and inorganic pollutants. Additionally, investigating *Pentaclethra macrophylla* pods' potential contributions to forming metallic composites or nanocomposites with other adsorbents holds promise.

Acknowledgements

We appreciate most sincerely the enormous gracious technical and other non-financial assistance received from the flagship Mentor-Mentee Research Program that was organized and executed by the Nigerian Academy of Science (NAS) with sponsorship from the UKAid and RISA.

Funding

This research did not receive any specific grant from funding agencies in the public, commercial, or not-for-profit sectors.

Conflict of Interests

The authors declare that they have no conflict of interest.

REFERENCES

Abugu, H. O., Okoye, P. A. C., Ajiwe, V. I. E., Omoku, P. E., & Umeobika, U. C. (2015). Preparation and characterization of activated carbon produced from oil Bean (Ugba or Ukpaka) and snail shell. *Journal of Environmental and Analytical Chemistry*, *26*. https://doi.org/http://dx.doi.org/10.4172/jreac.1000165

Ahmad, M. A., & Alrozi, R. (2011). Removal of malachite green dye from aqueous solution using rambutan peel-based activated carbon: Equilibrium, kinetic and thermodynamic studies. *Chemical Engineering Journal*, *171*(2), 510–516. https://doi.org/10.1016/j.cej.2011.04.018

Ahmad, M. A., Eusoff, M. A., Oladoye, P. O., Adegoke, K. A., & Bello, O. S. (2020). Statistical optimization of Remazol Brilliant Blue R dye adsorption onto activated carbon prepared from pomegranate fruit peel. *Chemical Data Collections*, *28*, 100426. https://doi.org/10.1016/j.cdc.2020.100426

Ajaelu, C. J., Oyedele, O., Ikotun, A. A., & Faboro, E. O. (2022). Safranin O dye removal using Senna fistula activated biomass: Kinetic, equilibrium and thermodynamic studies. *Journal of the Nigerian Society of Physical Sciences*, *5*, 951. https://doi.org/10.46481/jnsps.2023.951

Amin, M., Chung, E., & Shah, H. H. (2023). Effect of different activation agents for activated carbon preparation through characterization and life cycle assessment. *International Journal of Environmental Science and Technology*, *20*(7), 7645–7656. https://doi.org/10.1007/s13762-022-04472-6

Ao, W., Fu, J., Mao, X., Kang, Q., Ran, C., Liu, Y., Zhang, H., Gao, Z., Li, J., Liu, G., & Dai, J. (2018). Microwave assisted preparation of activated carbon from biomass: A review. In *Renewable and Sustainable Energy Reviews* (Vol. 92, Issue July 2017, pp. 958–979). Elsevier Ltd. https://doi.org/10.1016/j.rser.2018.04.051

ASTM D, 4607-94. (2006). *Standard Test Method for Determination of Iodine Number of Activated Carbon.* ASTM International.

Baba, E., Wyasu, G., Adefila, A. J., Dikko, N. A., & Yakasa, J. B. (2023). Production and characterization of activated carbon

derived from orange peel for the adsorption of methylene blue dye. *Science World Journal*, *18*(3), 492–498. https://doi.org/10.4314/swj.v18i3.25

Bade, M. M., Dubale, A. A., Bebizuh, D. F., & Atlabachew, M. (2022). Highly Efficient Multisubstrate Agricultural Waste-Derived Activated Carbon for Enhanced CO2 Capture. *ACE OMEGA*, *7*, 18770–18779. https://doi.org/https://doi.org/10.1021/aceomega.2c01528

Bello, O. S., Adegoke, K. A., & Akinyunni, O. O. (2017). Preparation and characterization of a novel adsorbent from Moringa oleifera leaf. *Applied Water Science*, *7*(3), 1295–1305. https://doi.org/10.1007/s13201-015-0345-4

Benadjemia, M., Millière, L., Reinert, L., Benderdouche, N., & Duclaux, L. (2011). Preparation, characterization and Methylene Blue adsorption of phosphoric acid activated carbons from globe artichoke leaves. *Fuel Processing Technology*, *92*(6), 1203–1212. https://doi.org/10.1016/j.fuproc.2011.01.014

Bouchelkia, N., Tahraoui, H., Amrane, A., Belkacemi, H., Bollinger, J. C., Bouzaza, A., Zoukel, A., Zhang, J., & Mouni, L. (2023). Jujube stones based highly efficient activated carbon for methylene blue adsorption: Kinetics and isotherms modeling, thermodynamics and mechanism study, optimization via response surface methodology and machine learning approaches. *Process Safety and Environmental Protection*, *170*(December 2022), 513–535. https://doi.org/10.1016/j.psep.2022.12.028

Cendekia, D., Ayu Afifah, D., & Hanifah, W. (2021). Linearity Graph in the Prediction of Granular Active Carbon (GAC) Adsorption Ability. *IOP Conference Series: Earth and Environmental Science*, *1012*(1). https://doi.org/10.1088/1755-1315/1012/1/012079

Chimi, T., Hannah, B. U., Lincold, N. M., Jacques, M. B., Tome, S., Hermann, D. T., Shikuku, V. O., Bissoue, A. N., Tchieta, G. P., & Meva, F. E. (2023). Preparation, characterization and application of H_3PO_4-activated carbon from Pentaclethra macrophylla pods for the removal of Cr(VI) in aqueous medium. *Journal of the Iranian Chemical Society*, *20*(2), 399–413. https://doi.org/10.1007/s13738-022-02675-9

Dai, F., Zhuang, Q., Huang, G., Deng, H., & Zhang, X. (2023). Infrared Spectrum Characteristics and Quantification of OH Groups in Coal. *ACS Omega*, *8*(19), 17064–17076. https://doi.org/10.1021/acsomega.3c01336

Ekpete, O. A., Marcus, A. C., & Osi, V. (2017). Preparation and Characterization of Activated Carbon Obtained from Plantain (Musa paradisiaca) Fruit Stem . *Journal of Chemistry*, *2017*, 1–6. https://doi.org/10.1155/2017/8635615

El-sayed, G. O., Yehia, M. M., & Asaad, A. A. (2014). Assessment of activated carbon prepared from corncob by chemical activation with phosphoric acid. *Water Resources and Industry*, *7–8*, 66–75. https://doi.org/10.1016/j.wri.2014.10.001

Faith, O. C., Nonso, U. C., Okechukwu, O., & Chukwuzuloke, O. C. (2017). Optimization and Characterization of Adsorptive Behavior of Pentaclethra macrophylla Activated Carbon on Aqueous Solution. *Sigma Journal of Engineering and Natural Sciences*, *35*(2), 213–226.

Gao, Y., Yue, Q., Gao, B., & Li, A. (2020). Insight into activated carbon from different kinds of chemical activating agents: A review. *Science of the Total Environment*, *746*, 141094. https://doi.org/10.1016/j.scitotenv.2020.141094

Genli, N., Kutluay, S., Baytar, O., & Şahin, Ö. (2022). Preparation and characterization of activated carbon from hydrochar by hydrothermal carbonization of chickpea stem: an application in methylene blue removal by RSM optimization. *International Journal of Phytoremediation*, *24*(1), 88–100. https://doi.org/10.1080/15226514.2021.1926911

Ghorbani, F., Kamari, S., Zamani, S., Akbari, S., & Salehi, M. (2020). Optimization and modeling of aqueous Cr(VI) adsorption onto activated carbon prepared from sugar beet bagasse agricultural waste by application of response surface methodology. *Surfaces and Interfaces*, *18*(January), 100444. https://doi.org/10.1016/j.surfin.2020.100444

Hidayu, A. R., & Muda, N. (2016). Preparation and Characterization of Impregnated Activated Carbon from Palm Kernel Shell and Coconut Shell for CO2Capture. *Procedia Engineering*, *148*, 106–113. https://doi.org/10.1016/j.proeng.2016.06.463

Iwar, R. T., Ogedengbe, K., & Ugwudike, B. O. (2022). Groundwater fluoride removal by novel activated carbon/aluminium oxide composite derived from raffia palm shells: Optimization of batch operations and field-scale point of use system evaluation. *Results in Engineering*, *14* (March), 100407. https://doi.org/10.1016/j.rineng.2022.100407

Jamnongkan, T., Intaramongkol, N., Kanjanaphong, N., Ponjaroen, K., Sriwiset, W., Mongkholrattanasit, R., Wongwachirakorn, P., Lin, K. Y. A., & Huang, C. F. (2022). Study of the Enhancements of Porous Structures of Activated Carbons Produced from Durian Husk Wastes. *Sustainability (Switzerland)*, *14*(10). https://doi.org/10.3390/su14105896

Jaria, G., Silva, C. P., Oliveira, J. A. B. P., Santos, S. M., Gil, M. V., Otero, M., Calisto, V., & Esteves, V. I. (2019). Production of highly efficient activated carbons from industrial wastes for the removal of pharmaceuticals from water—A full factorial design. *Journal of Hazardous Materials*, 212–218. https://doi.org/10.1016/j.jhazmat.2018.02.053

Jerônimo, D. P., De Souza, R. A., Da Silva, F. F., Camargo, G. L., Miranda, H. L., Xavier, M., Sakane, K. K., & Ribeiro, W. (2012). Detection of creatine in rat muscle by FTIR spectroscopy. *Annals of Biomedical Engineering*, *40*(9), 2069–2077. https://doi.org/10.1007/s10439-012-0549-9

Jiang, W., Xing, X., Li, S., Zhang, X., & Wang, W. (2019). Synthesis, characterization and machine learning based performance prediction of straw activated carbon. *Journal of Cleaner Production*, *212*, 1210–1223. https://doi.org/10.1016/j.jclepro.2018.12.093

Kalembkiewicz, J., Galas, D., & Sitarz-Palczak, E. (2018). The physicochemical properties and composition of biomass ash and evaluating directions of its applications. *Polish Journal of Environmental Studies*, *27*(6), 2593–2604. https://doi.org/10.15244/pjoes/80870

Karim, A. Y. A., Balogoun, C., Avocefohoun, A. S., Prodjinonto, V., Gbaguidi, M. A. N., Dovonon, L. F., Saizonou, M., Agossou, G., Djihouessi, B., Sogbochi, E., Aïna, M., Alitonou, G. A., & Sohounhloue, D. C. K. (2022). Influence of Some Preparation Parameters on The Efficiency of Activated Carbons Prepared from Teak Wood Shavings (Tectona Grandis) and Coconut Shells (Cocos Nucifera) for The Treatment of Industrial Wastewater. *European Journal of*

Advanced Chemistry Research, *3*(4), 1–9. https://doi.org/10.24018/ejchem.2022.3.4.121

Kurian, J. K., Gariepy, Y., Orsat, V., & Raghavan, G. S. V. (2015). Microwave-assisted lime treatment and recovery of lignin from hydrothermally treated sweet sorghum bagasse. *Biofuels*, *6*(5–6), 341–355. https://doi.org/10.1080/17597269.2015.1110775

Kurisingal, J. F., Yun, H., & Hong, C. S. (2023). Porous organic materials for iodine adsorption. *Journal of Hazardous Materials*, *458*(March), 131835. https://doi.org/10.1016/j.jhazmat.2023.131835

Kwiatkowski, M., & Broniek, E. (2017). An analysis of the porous structure of activated carbons obtained from hazelnut shells by various physical and chemical methods of activation. *Colloids and Surfaces A: Physicochemical and Engineering Aspects*, *529*. https://doi.org/10.1016/j.colsurfa.2017.06.028

Lam, S. S., Liew, R. K., Wong, Y. M., Yek, P. N. Y., Ma, N. L., Lee, C. L., & Chase, H. A. (2017). Microwave-assisted pyrolysis with chemical activation, an innovative method to convert orange peel into activated carbon with improved properties as dye adsorbent. *Journal of Cleaner Production*, *162*. https://doi.org/10.1016/j.jclepro.2017.06.131

Li, S., Han, K., Li, J., Li, M., & Lu, C. (2017). Preparation and characterization of super activated carbon produced from gulfweed by KOH activation. *Microporous and Mesoporous Materials*, *243*, 291–300. https://doi.org/10.1016/j.micromeso.2017.02.052

Liew, R. K., Azwar, E., Yek, P. N. Y., Lim, X. Y., Cheng, C. K., Ng, J. H., Jusoh, A., Lam, W. H., Ibrahim, M. D., Ma, N. L., & Lam, S. S. (2018). Microwave pyrolysis with KOH/NaOH mixture activation: A new approach to produce micro-mesoporous activated carbon for textile dye adsorption. *Bioresource Technology*, *266*. https://doi.org/10.1016/j.biortech.2018.06.051

Loredo-Cancino, M. Soto-Regaldo, E. Cerino-Corfova, F.J. Garcia-Reyes, R.B., Garcia-Leon, A.M. and Garza-Gonzalez, M. T. (2013). Determining optimal conditions to produce activated carbon from barley husks using single or dual optimization. *Journal of Environmental Management*, *125*, 117–125. https://doi.org/10.1016/j.jenvman.2013.03.028

Montgomery, D. C. (2017). *Desgin And Analysis Of Experiments*.

Montoya-Suarez, S., Colpas-Castillo, F., Meza-Fuentes, E., Rodríguez-Ruiz, J., & Fernandez-Maestre, R. (2016). Activated carbons from waste of oil-palm kernel shells, sawdust and tannery leather scraps and application to chromium(VI), phenol, and methylene blue dye adsorption. *Water Science and Technology*, *73*(1), 21–27. https://doi.org/10.2166/wst.2015.293

Ngueabouo, A. M. S., Tagne, R. F. T., Tchuifon, D. R. T., Fotsop, C. G., Tamo, A. K., & Anagho, S. G. (2022). Strategy for optimizing the synthesis and characterization of activated carbons obtained by chemical activation of coffee husk. *Materials Advances*, *3*(22), 8361–8374. https://doi.org/10.1039/d2ma00591c

Nindjio, G. F. K., Tagne, R. F. T., Jiokeng, S. L. Z., Fotsop, C. G., Bopda, A., Doungmo, G., Temgoua, R. C. T., Doench, I., Njoyim, E. T., Tamo, A. K., Osorio-Madrazo, A., & Tonle, I. K. (2022). Lignocellulosic-Based Materials from Bean and Pistachio Pod Wastes for Dye-Contaminated Water Treatment: Optimization and Modeling of Indigo Carmine Sorption. *Polymers*, *14*(18). https://doi.org/10.3390/polym14183776

Ogbeh, G. O., & Ominiyi, D. A. (2022). The Optimal Performances of Starches from two Cassava varieties as Bioflocculants for the Treatment of Textile Wastewater. *Pollution*, *8*(4), 1369–1386. https://doi.org/10.22059/POLL.2022.339603.1381

Ogungbenro, E.A., Quang, V.D., Al-Ali, K. and Abu-Zahra, R. M. M. (2017). Activated carbon from date seeds for CO2 capture applications. *Energy Procedia (13th International Conference on Green Gas Control Technologies GHGT-13, Lausanne, Switzerland)*, *114*, 2313–2321. https://doi.org/doi: 10.1016/j.egypro.2017.03.1370

Okey-Onyesolu, C. ., Okoye, C. ., & Chime, D. . (2018a). Removal of Eosin yellow dye from aqueous solution using oil bean seed shells based activated carbons: Equilibrium, Kinetics and thermodynamics studies. *International Journal of Scientific & Engineering Research*, *9*(3), 140–167.

Okey-Onyesolu, C. F., Okoye, C. C., & Chime, D. C. (2018b). Removal of Eosin yellow dye from aqueous solution using oil bean seed shells based activated carbons: Equilibrium, Kinetics and thermodynamics studies. *International Journal of Scientific & Engineering Research*, *9*(3), 140–167.

Okpala, B. (2015). 18 reasons why you need the African oil bean (Ukpaka or Ugba). *Global Food Book*.

Onija, O., Borodi, G., Kacso, I., Pop, M. N., Dadarlat, D., Bratu, I., & Jumate, N. (2012). Preparation and characterization of urea-oxalic acid solid form. *AIP Conference Proceedings*, *1425*(1), 35–38. https://doi.org/10.1063/1.3681960

Pongener, C., Kibami, D., Rao, K. S., Goswamee, R. L., & Sinha, D. (2015). Synthesis and Characterization of Activated Carbon from the Biowaste of the Plant Manihot Esculenta. *Chemical Science Transactions*, *4*(1), 59–68. https://doi.org/10.7598/cst2015.958

Putranto, A., Ng, Z. W., Hadibarata, T., Aziz, M., Yeo, J. Y. J., Ismadji, S., & Sunarso, J. (2022). Effects of pyrolysis temperature and impregnation ratio on adsorption kinetics and isotherm of methylene blue on corn cobs activated carbons. *South African Journal of Chemical Engineering*, *42*(July), 91–97. https://doi.org/10.1016/j.sajce.2022.07.008

Ravichandran, P., Sugumaran, P., Seshadri, S., & Basta, A. H. (2018). Optimizing the route for production of activated carbon from Casuarina equisetifolia fruit waste. *Royal Society Open Science*, *5*(7). https://doi.org/10.1098/rsos.171578

Sarma, P. J., Kumar, R., & Pakshirajan, K. (2015). Batch and continuous removal of copper and lead from aqueous solution using cheaply available agricultural waste materials. *International Journal of Environmental Research*, *9*(2), 635–648.

Shamsuddin, M. S., Yusoff, N. R. N., & Sulaiman, M. A. (2016). Synthesis and characterization of activated carbon produced from kenaf core fiber using H3PO4 activation. *Procedia Chemistry*, *19*, 558–565. https://doi.org/10.1016/j.proche.2016.03.053

Stoycheva, I., Petrova, B., Tsyntsarski, B., Dolashka, P., Kosateva, A., & Petrov, N. (2023). Investigation of the Adsorption Process of Triclosan from an Aqueous Solution, Using Nanoporous Carbon Adsorbents, Obtained after Treatment of Organic Household and Vegetable Waste. *Processes*,

DOI: https://dx.doi.org/10.4314/swj.v18i4.22

11, 2643. https://doi.org/https://doi.org/10.3390/pr11092643

Thongpat, W., Taweekun, J., & Maliwan, K. (2021). Synthesis and characterization of microporous activated carbon from rubberwood by chemical activation with KOH. *Carbon Letters*, *31*(5), 1079–1088. https://doi.org/10.1007/s42823-020-00224-z

Van, K. Le, & Thu, T. L. T. (2019). Preparation of pore-size controllable activated carbon from rice husk using dual activating agent and its application in supercapacitor. *Journal of Chemistry*, *2019*. https://doi.org/10.1155/2019/4329609

Vunain, E., Njewa, J. B., Biswick, T. T., & Ipadeola, A. K. (2021). Adsorption of chromium ions from tannery effluents onto activated carbon prepared from rice husk and potato peel by H3PO4 activation. *Applied Water Science*, *11*(9), 1–14. https://doi.org/10.1007/s13201-021-01477-3

Wang, W., Xu, S., Wang, K., Liang, J., & Zhang, W. (2019). De-intercalation of the intercalated potassium in the preparation of activated carbons by KOH activation. *Fuel Processing Technology*, *189*(February), 74–79. https://doi.org/10.1016/j.fuproc.2019.03.001

Xu, T., Qiu, X., Zhang, X., & Xia, Y. (2023). Regulation of surface oxygen functional groups and pore structure of bamboo-derived hard carbon for enhanced sodium storage performance. *Chemical Engineering Journal*, *452*(P4), 139514. https://doi.org/10.1016/j.cej.2022.139514

Yang, K., Peng, J., Srinivasakannan, C., Zhang, L., Xia, H., & Duan, X. (2010). Bioresource Technology Preparation of high surface area activated carbon from coconut shells using microwave heating. *Bioresource Technology*, *101*(15), 6163–6169. https://doi.org/10.1016/j.biortech.2010.03.001

Yashim, M. M., Razali, N., Saadon, N., & Rahman, N. A. (2016). Effect of activation temperature on properties of activated carbon prepared from oil palm kernel shell (OPKS). *ARPN Journal of Engineering and Applied Sciences*, *11*(10), 6389–6392.

Yokoyama, J. T. C., Cazetta, A. L., Bedin, K. C., Spessato, L., Fonseca, J. M., Carraro, P. S., Ronix, A., Silva, M. C., Silva, T. L., & Almeida, V. C. (2019). Stevia residue as new precursor of CO2-activated carbon: Optimization of preparation condition and adsorption study of triclosan. *Ecotoxicology and Environmental Safety*, *172*(December 2018), 403–410. https://doi.org/10.1016/j.ecoenv.2019.01.096

Yorgun, S., & Yildiz, D. (2015). Preparation and characterization of activated carbons from Paulownia wood by chemical activation with H3PO4. *Journal of the Taiwan Institute of Chemical Engineers*, *53*, 122–131. https://doi.org/10.1016/j.jtice.2015.02.032

Zakaria, R., Jamalluddin, N. A., & Abu Bakar, M. Z. (2021a). Effect of impregnation ratio and activation temperature on the yield and adsorption performance of mangrove based activated carbon for methylene blue removal. *Results in Materials*, *10*(March), 100183. https://doi.org/10.1016/j.rinma.2021.100183

Zakaria, R., Jamalluddin, N. A., & Abu Bakar, M. Z. (2021b). Effect of impregnation ratio and activation temperature on the yield and adsorption performance of mangrove based activated carbon for methylene blue removal. *Results in Materials*, *10*(April), 100183. https://doi.org/10.1016/j.rinma.2021.100183

Zhang, S., Sun, S., Gao, N., Quan, C., & Wu, C. (2022). Effect of auto thermal biomass gasification on the sintering of simulated ashes. *Applications in Energy and Combustion Science*, *9*, 100054. https://doi.org/10.1016/j.jaecs.2021.100054

Zhao, C., Ge, L., Zuo, M., Mai, L., Chen, S., Li, X., Li, Q., Wang, Y., & Xu, C. (2023). Study on the mechanical strength and iodine adsorption behavior of coal-based activated carbon based on orthogonal experiments. *Energy*, *282*(April), 128450. https://doi.org/10.1016/j.energy.2023.128450

Zieliński, B., Miądlicki, P., & Przepiórski, J. (2022). Development of activated carbon for removal of pesticides from water: case study. *Scientific Reports*, *12*(1), 1–14. https://doi.org/10.1038/s41598-022-25247-6

Zięzio, M., Charmas, B., Jedynak, K., Hawryluk, M., & Kucio, K. (2020). Preparation and characterization of activated carbons obtained from the waste materials impregnated with phosphoric acid(V). *Applied Nanoscience (Switzerland)*, *10*(12), 4703–4716. https://doi.org/10.1007/s13204-020-01419-6